ISSN 1054-660X, Laser Physics, 2011, Vol. 21, No. 3, pp. 601–607.

Towards Quantitative Acousto-Optic Imaging in Tissue[1]

A. Bratchenia*, R. Molenaar, and R. P. H. Kooyman

Faculty of Science and Technology, MIRA Institute University of Twente P.O. Box 217, 7500AE Enschede, the Netherlands

*e-mail: a.bratchenia@tnw.utwente.nl

Received April 22, 2010; in final form, August 24, 2010; published online February 2, 2011

Abstract—We have investigated the possibilities and limitations of the application of ultrasound modulated coherent light to obtain quantitative information of local absorbers in light-scattering objects, among which tissue. For all objects studied, the combined use of microsecond ultrasound and light pulses enabled us to construct a 3D map of local absorbers with a spatial resolution of ~2 mm. Moreover, in relatively homogeneous model systems, mimicking a blood vessel embedded in tissue, the use of a calibration procedure allowed for a determination of the local absorbance. Speckle decorrelation times for real tissue containing blood vessels, in which appreciable motion of scatterers can exist, were found to be smaller than 1ms. These relatively short times present a major challenge for acousto-optics to be applied in living tissue systems.

DOI: 10.1134/S1054660X11050033

INTRODUCTION

The exploitation of light-tissue interaction for biomedical purposes is a research area of great scientific and societal interest, owing to their relatively inexpensive instrumentation that is required (as opposed to MRI); furthermore, moderate light intensities are harmless to tissue (as opposed to, e.g., X-ray tomography). Approaches such as laser Doppler methods, diffuse optical tomography are finding their way to real-world applications [1].

However, a serious limitation is that light with a wavelength within the tissue window ($\lambda \sim 500$–1500 nm) is heavily scattered by tissue, which prevents in many cases measurements deep in tissue. Also, the ill-defined optical path lengths in such systems preclude quantification of local optical properties, such as specific absorbances. There are several approaches to address this shortcoming, among which the combination of ultrasound (US) and optics appears to be the most promising: US is hardly scattered by tissue, implying that it can be used to define the region of interest in tissue. One widely investigated US-optics combination is photoacoustics (PA) where a short intense laser pulse is applied to tissue (e.g., [2, 3]). In regions where the light is absorbed a heat pulse is generated that translates into a pressure pulse. Using an acoustic detector the origin of this pressure pulse can be detected with sub-millimeter resolution. However, a quantitative interpretation of PA responses in terms of local absorbances is hampered by the fact that it is difficult to quantify the local light fluence.

A more recent approach, acousto-optics (AO), appears to be more promising in this respect. In this paper we will focus upon the prospects and challenges that are met in developing AO for quantitative tissue imaging.

[1] The article is published in the original.

USING ACOUSTO-OPTICS FOR IMAGING

Contrary to PA in AO spatial information is obtained by interrogating the structure of interest simultaneously with ultrasound and light, whereas an optical response is detected. An in-depth discussion of the mechanisms of AO modulation is given by Wang [4]. In short, an acoustic periodic disturbance with frequency f induces in the structure under investigation (1) a periodic compression/expansion of the medium resulting in a modulation of the refractive index; (2) a periodic movement of scatter particles present within the structure. If simultaneously a coherent light beam is sent through the structure, the speckle pattern will be modulated as a result of these disturbances, which can be detected by, e.g., a CCD camera [5]. The net result is that the light that has traversed the ultrasound-irradiated volume has been labeled with the ultrasound frequency.

An important advantage of such a hyphenated approach is that acoustics defines the region of interest and optics provides us with spectral information on this region; contrary to PA the detected response can be relatively simply interpreted in terms of local absorbances. We have previously shown [6] that for a 2D system the use of μs-US-pulses at $f = 2.25$ MHz in combination with laser pulses allows us to quantitatively determine the absorption coefficient in a scattering volume with a spatial resolution of $\sim 2 \times 2 \times 2$ mm^3.

To extend this approach to map 3D structures it suffices to perform a planar scan with the US-source over the region of interest.

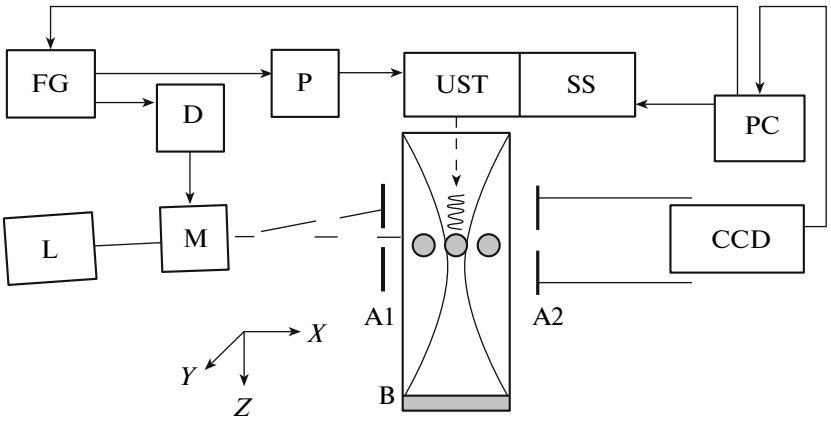

Fig. 1. Schematics of the acousto-optical setup in transmission geometry. FG: 2-channel programmable function generator (Tektronix AFG3102). D: delay line. P: MOSFET pulser to drive transducer. UST: 2.25 MHz ultrasound transducer (Panametrics V309). L: laser, M: acousto optical modulator (Isomet 1201E-1). Al: aperture to block non-deflected light. A2: aperture. B: IL-based phantom. CCD: camera Basler A102f (12bits, 1392 × 1040). In the center of the phantom the cross-section of an absorber containing tube is depicted. The US-propagation is along the *Z*-direction.

An issue, specific to AO, is that of speckle decorrelation. Essential for successful AO experiments is that the speckle pattern modulation is predominantly induced by the acoustic disturbance. This implies (1) that the used light source should be sufficiently coherent, and (2) that for a meaningful AO signal a measurement has to be completed within a time where Brownian motion of scatterers is insignificant.

MATERIALS AND METHODS

Objects for Measurement

To investigate various aspects of AO imaging we have prepared several objects, all of which reflect some property of real tissue.

Cylindrical object(s). As a basic model for an absorber containing tissue we used a Perspex container (*XYZ*-dimensions ~20 × 45 × 40 mm^3) filled with an Intralipid solution in an Agar matrix [7], with a reduced scattering coefficient $\mu_s' \sim 1.95$ mm^{-1} at $\lambda =$ 514 nm, i.e., similar to that of tissue. Perpendicular to the *X*-axis, with their axes along *Y* (cf. Fig. 1), two silicone tubes were mounted in the center of the container. Inner diameter of the tubes was 3 mm, their walls had a thickness of 0.5 mm. Their wall-to-wall distance was approximately 8 mm. The tubes could be filled with absorbers of predefined absorbances that were embedded in either an Agar/Intralipid mixture or in a yoghurt/milk mixture. Such an assembly can be considered as a simple model system for blood vessels present in tissue.

Spherical objects. In another series small spherical objects with a diameter of 1.5 mm and with a known absorbance were buried in a cylindrical container with its symmetry-axis along *Z*, filled with a Agar/Intralipid mixture. The diameter of the cylinder is 28 mm.

Real tissue. As a more realistic system we also used a fresh piece of chicken-breast tissue, in which absorbing spheres of ~1.5 mm in diameter were buried.

Acousto-Optics Setup

In Fig. 1 the schematics of the setup is depicted. Prior to AO experiments the positions of the absorbing structures, either within the tubes or within the chicken tissue were determined using a commercial US pulser-receiver (Panametrics 5077PR). High pressure (~1.5 MPa) US- bursts with a length ~ 1 μs, produced by a 2.25 MHz ultrasound transducer, were sent along the *Z*-axis of the container. The focal point of the US-bursts was chosen such that it coincided with the known positions of the absorbers; these bursts resulted in an effective US disturbance volume of ~2 × 2 × 3 mm^3 around the focal center. The transducer was mounted on a computer-controlled XY translation stage with sub-mm resolution. Acoustic coupling between transducer and the system under investigation was accomplished by a water layer.

As light sources two laser systems were available: a 260 mW Argon laser, operating at $\lambda = 514$ nm, and a CW Ti-sapphire laser (600 mW at $\lambda = 750$ nm), respectively.

Light pulses of ~1 μs duration, entering the sample along the *X*-axis, were produced by deflection of the laser beam by an acousto-optic modulator. The delay time of the laser pulse relative to the start of the US burst could be set in the range 2–25 μs. The coherent light traveling through the sample produced a speckle pattern that was detected by a CCD-camera. Using a 6 mm diameter diaphragm, placed close to the sample, the distance between camera and sample was set such that approximately one speckle illuminated one cam-

era pixel. Laser beam, diaphragm and camera axis were approximately in line.

EXPERIMENTS AND DATA TREATMENT

The delay time between laser pulse and US burst determined the Z-position of the sample where the acoustic disturbance was measured. By varying this delay a Z-scan of the sample was performed. By translating the US transducer in the XY-plane a 3D-scan of the complete volume could be measured.

A convenient way of recording the AO response is by measuring the speckle contrast as measured by the camera: a US-induced oscillating speckle pattern results in a blurred speckle image, provided the exposure time (milliseconds range) is larger than the period of the speckle modulation (microseconds range). The consequence is a decreased contrast of the speckle image. A typical contrast profile resulting from an AO experiment is depicted in Fig. 2, where a 3 mm absorber-containing tube is buried within an Agar/Intralipid mixture. It is seen that around a position $z \approx 22.5$ mm, where the absorber is located, the contrast is at maximum: in this region most photons are absorbed and consequently US-induced speckle oscillations are hardly present. From the figure we can also estimate the Z-resolution that can be obtained: judging by the half width of the central peak a resolution of ~2 mm is found.

For this type of detection approach, it is essential that within the camera exposure time random speckle fluctuations due to Brownian motion are nearly absent, while simultaneously sufficient photons are collected for a satisfactory signal-to-noise ratio (SNR).

For the majority of samples that we investigated a reasonable balance was found by accumulating at each US position hundreds of light/US exposure cycles with a camera exposure time of 50 ms for each cycle. The analysis of the camera's raw images is carried out by determining the speckle contrast $C(z)$:

$$C(z) = \frac{\sigma}{\mu}, \tag{1}$$

where σ is the standard deviation of the pixel values of an image and μ is the mean pixel value.

Because our main interest is the relative change of $C(z)$ when US is applied, we define the modulation depth $M(z)$:

$$M(z) = \frac{\Delta C(z)}{C(z)} \tag{2}$$

with $\Delta C = C_b - C$, and C_b the background contrast when no ultrasound is present.

We have previously shown [6, 8] that the introduction of a normalized modulation depth M_{norm}, together with a calibration procedure based upon a modified Lambert–Beer law, allows us to interpret

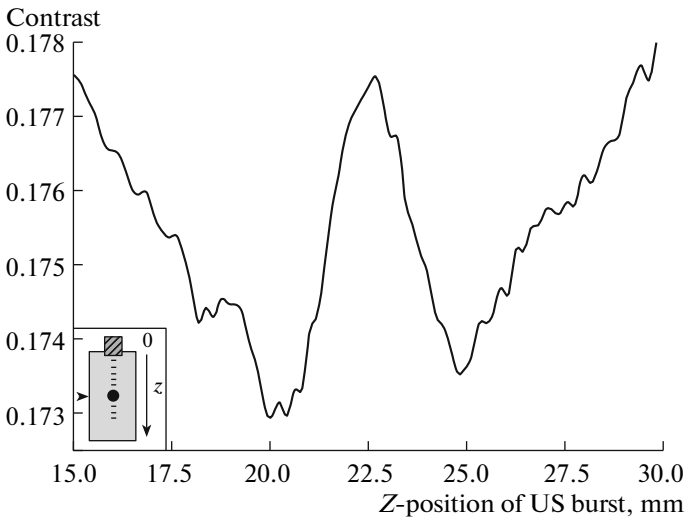

Fig. 2. Dependence of contrast profile on the Z-axis position of US burst in the presence of an absorber at $z \approx 22.5$ mm. The width of the absorber is ≈3 mm. Contrast profile is spline interpolated.

experimental data in terms of local absorbances, where M_{norm} is defined as:

$$M_{\text{norm}} = \frac{M(\mathbf{r}, \lambda)}{M_{\mu a = 0}(\mathbf{r}, \lambda)}. \tag{3}$$

Here, M is the modulation depth when an optical absorber is present, and $M_{\mu a = 0}$ is M measured in the absence of an optical absorber in the US path. $\mathbf{r}$ is the position of the center of the US modulation zone.

The calibration is carried out by determining M for a set of absorbers of known absorbance. It turned out [8] that this procedure allowed us to determine the concentration ratio of two different absorbers to within ~15%.

The normalization/calibration procedure gives the outlook to determine absorbances irrespective of their position within the interrogated structure [9].

In addition to AO experiments we have also carried out homodyne dynamic light scattering experiments using a nanosecond correlator (Flex 02-08DC) in combination with an avalanche photodiode (SPCM AQR13).

RESULTS AND DISCUSSION

Imaging

In Fig. 3 the raw modulation depth values maps are shown for the system where one tubes was embedded, one for the situation with the tube filled with an absorbing scattering medium with $\mu_a \approx 0.27$ mm^{-1} at $\lambda = 514$ nm (Fig. 3a), and another one where the tube contained only the scattering medium (Fig. 3b). From a comparison of the two figures it is seen that there is only faint evidence for an absorbing structure within

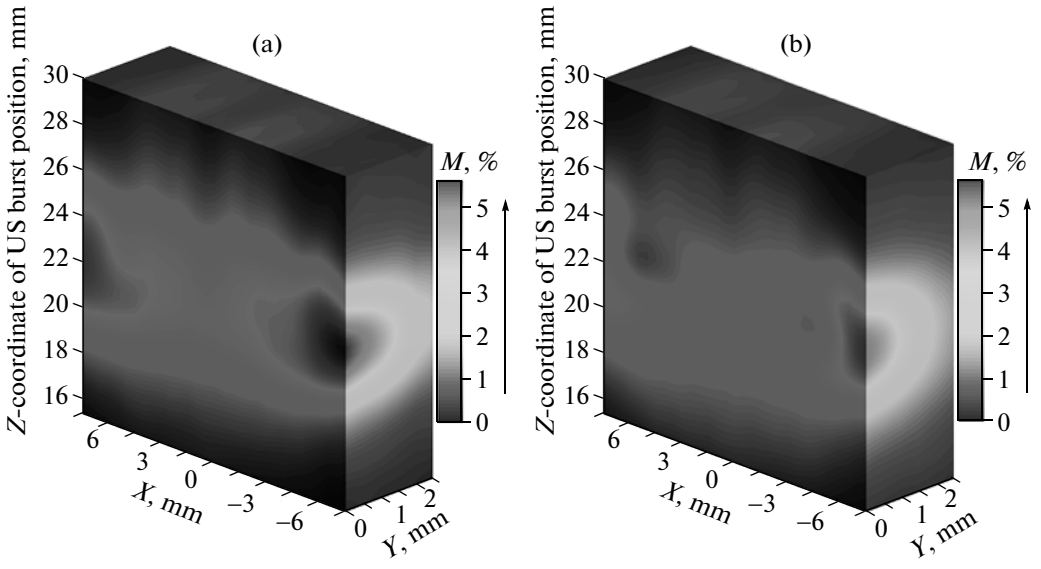

Fig. 3. Modulation depth M of an object (a) without, and (b) with absorbing inclusion respectively. The figures were constructed from datasets containing 186 *Z*-scans which took ~286 minutes to complete. Scanning step size: 0.375 mm in the *Z* direction and 0.5 mm in the *X*–*Y* directions. Scanning range: 35 mm in the *Z* direction, 15 mm in *X* direction and 2.5 mm in the *Y* direction.

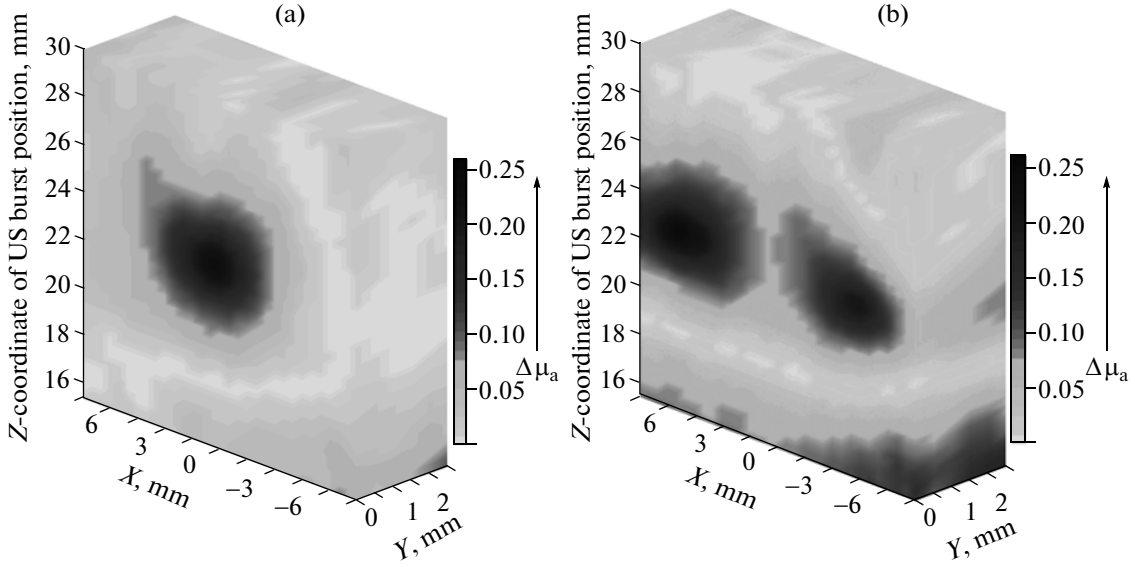

Fig. 4. The *X* axis cross-section of the map of μ_a values. *X*, *Y* are the coordinates of the US transducer. Light is entering the phantom from the right, (a) one embedded tube; (b) two embedded tubes.

the system. However, if we perform the normalization step of Eq. (3), the cylindrical absorbing structure is clearly revealed (Fig. 4a). Moreover, by applying the calibration data we can convert the map of modulation depths into a map of absorption coefficients, as is seen in Fig. 4a. The same procedure can be applied to a more complex geometry: in the situation of Fig. 4b two absorber containing tubes were embedded. In this figure, where the light is traveling in the positive direction of the *X*-axis, the set value of μ_a in the tube centered at $x \approx 6$ mm is closely reproduced, whereas that of the second tube exhibits a somewhat lower value. Apparently, the used normalization step cannot fully account for the variation in the photon density: in principle, the distribution of the photon density over the *complete* system under investigation is affected by the presence of a second absorber. Nevertheless, it is striking that this circumstance has only limited impact on the quantitative determination of a position resolved absorption coefficient. However, we expect that for more complicated systems this effect will be more serious; to completely solve this shortcoming

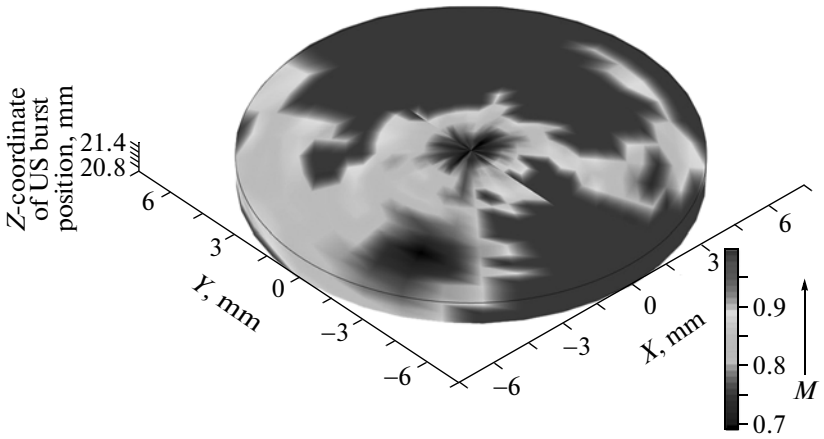

Fig. 5. The map of M_{norm} values depending on the X and Y axes coordinates of the US transducer. There are three absorbing beads inside the phantom. As there is an experimentally found accuracy of ~10% in M values, those in the range of 0.95–1.10 are set to 1.

tomography methods should be applied, e.g., by rotating the light source and detector around the objects of interest.

A first step to such an approach is depicted in Fig. 5, where the left panel shows a top-view photograph of the investigated structure, and the right panel is a 2D map of measured M_{nom}-values, obtained by rotating the object between light source and detector with 19 angular steps of 10°, and translating the US transducer along X in 0.5 mm steps. In fact, Fig. 5b is a map of photon densities; we clearly see the shadows caused by the presence of the absorbers. We see that the diameter of the absorbing spheres (~1.5 mm) is reasonably well reproduced. However, it is also obvious that the presence of the shadows prohibits the detection of smaller absorbances and/or absorbers.

It is expected that real biological tissue will be much less homogeneous than the systems we considered until now. In Fig. 6 we show the M_{norm}-map of chicken-breast tissue in which a cluster of 3 absorbers of 1.5 mm diameter with mutual distances of <1 mm was buried (for details see figure captions). The use of a Ti-sapphire laser operating at $\lambda = 150$ nm permitted us to work within the tissue window. Again, the presence of the cluster is well revealed, and the spatial resolution is similar to that found in the more simple systems. However, we failed to resolve the individual absorbers, which we attribute partly to the relatively large inhomogeneity of the surrounding tissue. Using a higher US frequency we expect that the resolution can be somewhat improved. It has to be added that with the current calibration method a quantitative interpretation is out of reach. To circumvent the calibration procedure one of the options is to solve the inverse problem by using the diffusion approximation to the radiative transfer equation [10]. This approach will be published elsewhere [11].

SPECKLE DECORRELATION

In table approximate speckle decorrelation times are given for a number of objects investigated. The data were obtained by measuring the intensity correlation function in a classical homodyne dynamic light scattering experiment. Note that these data were acquired without applying US.

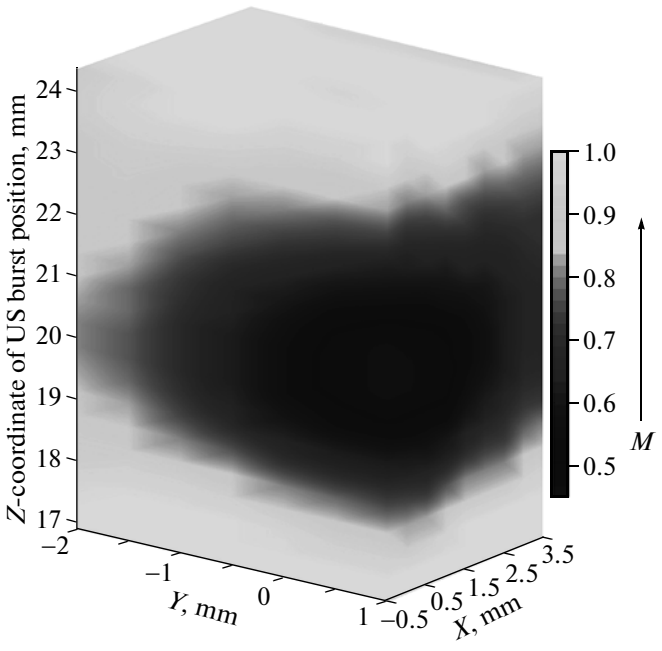

Fig. 6. The X axis cross-section of the map of M_{norm} values. X, Y are the coordinates of the US transducer. Light is entering the chicken breast tissue from the right. Three absorbing beads of $\mu_a \approx 0.6$ mm^{-1} are placed in the tissue.

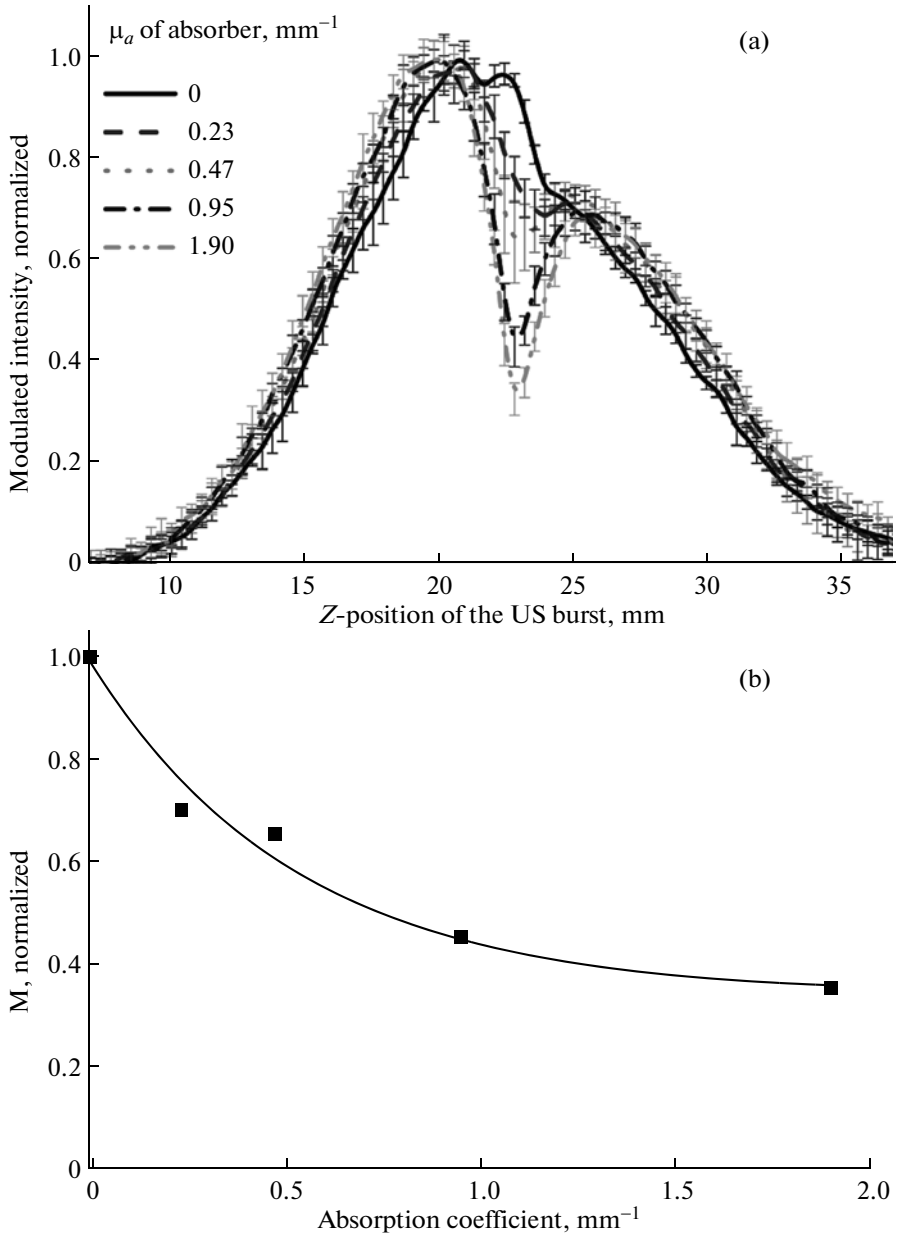

Fig. 7. (a) M_{norm} profile as a function of the Z-position of US burst for an IL phantom with an absorber prepared by mixing yogurt, milk and dye. CCD exposure time is 3 ms, corresponding to a speckle decorrelation time of the sample. The width of the absorber is ≈1.5 mm. The net measuring time for one profile is ~1 min. Profile is spline interpolated. (b) Measured values of M_{norm} at Z ~ 22.5 mm plotted as a function of μ_a. The line is a single-exponential fit.

As the AO experiment is an essentially low light-level experiment, this table illustrates an important issue: as already mentioned the measurement approach relies upon recording the contrast decrease as a result of AO disturbances- any contrast decrease due to other causes will affect the SNR. This implies that a complete single cycle measurement should be accomplished within roughly two times the decorrelation time τ, in the present context defined as the time where the correlation function has decreased to half its initial value. Within this time sufficient photons should have been collected for a meaningful determination of the contrast. From the table we conclude that applying AO to living tissue demands net measuring times not larger than a few milliseconds.

In Fig. 7a results are shown obtained from AO experiments carried out on a system consisting of the previously described rectangular container where a 3 mm inner diameter tube was filled with a *mobile* absorber, prepared by adding a dye to a yoghurt/milk mixture. As indicated in table the complete system had a speckle decorrelation time of ~2 ms. This can be con-

Speckle correlation times for a number of objects. Except for those in living tissue, correlation times were obtained for material placed in the basic rectangular container. The arm was measured in reflection mode

Object	Correlation time τ, ms
Milk	<1
Milk/yoghurt 1 : 1	2
IL/Agar	30
Arm	1
Fingertip	<1

sidered as a model system for a blood vessel in tissue. The use of a powerful Ti-sapphire laser permitted us to reduce the net single cycle measuring time to ~4 ms, with the result that indeed M_{norm} can be determined as a function of the local μ_a. In Fig. 7b we have plotted the found M_{norm}-values as a function of μ_a, and fitted the data to a Lambert–Beer type model, as described in our previous work [6]. Although the number of data points is somewhat scarce, the quality of the fit is reasonable (correlation coefficient 0.98). Moreover, we found an effective optical path length to be ~2 mm, similar to that found in earlier experiments with the same tube diameter [6]. These findings make us to conclude that with the current experimental approach quantitative measurements on the oxygenation degree in blood vessels with a diameter ~1–3 mm appear to be within reach.

CONCLUSIONS

We have shown that for a number of different systems that mimic tissue the presence of absorbers can be located with a spatial resolution of ~2 mm. For relatively homogeneous systems local absorbances can be semi-quantitatively determined using a normalization/calibration procedure. However, extension to tomography, together with the application of more elaborate mathematical methods is required for a fully quantitative description in more complex systems.

As AO is a coherent technique, based upon the analysis of time-dependent speckle-statistics, the major challenge for its application in real tissue is to overcome the speckle decorrelation due to internal Brownian motion. One approach, the use of a nanosecond-range correlator [12], is essentially independent of speckle decorrelation, but severely lacks SNR because its output depends on the analysis of one single speckle. Another method, heterodyne interferometry, promises to increase SNR with an order of magnitude [13]. However, this method has the drawback of a complicated setup. Although other approaches have been suggested [14], none of them has emerged as the ultimate solution. Alternatively, one could try to decrease the optical path length by working in reflection mode. However, this results in a situation where only superficial structures can be investigated.

It remains for the near future to decide which of these options are practical for measurements of real tissue.

ACKNOWLEDGMENT

This research was supported by the Dutch Technical Science Foundation (STW), project no. TGT.6656.

REFERENCES

1. *Handbook of Optical Biomedical Diagnostics*, Ed. by V. Tuchin (SPIE Press, Washington, 2002).
2. M. Xu and L.-H. V. Wang, Rev. Sci. Instrum. **77**, 041101 (2006).
3. G. Giubileo, A. Puiu, F. Dell'Unto, M. Tomasi, and A. Fagnani, Laser Phys. **19**, 245 (2009).
4. L.-H. V. Wang, Phys. Rev. Lett. **87**, 043903 (2001).
5. J. Li, G. Ku, and L.-H. V. Wang, Appl. Opt. **41**, 6030 (2002).
6. A. Bratchenia, R. Molenaar, and R. P. H. Kooyman, Appl. Phys. Lett. **92**, 113901 (2008).
7. R. Cubeddu, A. Pifferi, P. Taroni, A. Torricelli and G. Valentini, Phys. Med. Biol. **42**, 1971 (1997).
8. A. Bratchenia, R. Molenaar, T. G. van Leeuwen, and R. P. H. Kooyman, J. Biomed. Opt. **14**, 4031 (2009).
9. A. Bratchenia, R. Molenaar, and R. P. H. Kooyman, Proc. SPIE **7177**, 71771H (2009).
10. A. P. Gibson, J. C. Hebden, and S. R. Arridge, Phys. Med. Biol. **50**, R1 (2005).
11. A. Bratchenia, R. Molenaar, T. G. van Leeuwen, and R. P. H. Kooyman (in preparation).
12. A. Bratchenia, R. Molenaar, and R. P. H. Kooyman, Proc. SPIE **6437**, 64371P (2007).
13. M. Atlan, B. C. Forget, F. Ramaz, and A. C. Boccara, Opt. Lett. **30**, 1360 (2005).
14. L. Sui, T. Murray, G. Maguluri, A. Nieva, F. Blonigen, C. DiMarzio, and R. A. Roy, Proc. SPIE **5320**, 164 (2004).